

# Extensive Natural Variation for Cellular Hydrogen Peroxide Release Is Genetically Controlled

Homa Attar<sup>1\*</sup>, Karen Bedard<sup>2#a</sup>, Eugenia Migliavacca<sup>1,3</sup>, Maryline Gagnebin<sup>1</sup>, Yann Dupré<sup>1</sup>, Patrick Descombes<sup>4#e</sup>, Christelle Borel<sup>1#b</sup>, Samuel Deutsch<sup>1#c</sup>, Holger Prokisch<sup>5</sup>, Thomas Meitinger<sup>5</sup>, Divya Mehta<sup>5#d</sup>, Erich Wichmann<sup>5,6,7</sup>, Jean Maurice Delabar<sup>8</sup>, Emmanouil T. Dermitzakis<sup>1</sup>, Karl-Heinz Krause<sup>2</sup>, Stylianos E. Antonarakis<sup>1\*</sup>

**1** Department of Genetic Medicine and Development, University of Geneva Medical School, Geneva, Switzerland, **2** Department of Pathology and Immunology, University of Geneva Medical School and University Hospitals, Geneva, Switzerland, **3** Swiss Institute of Bioinformatics, University of Lausanne, Dorigny, Switzerland, **4** Genomics Platform, NCCR Frontiers in Genetics, University of Geneva Medical School, Geneva, Switzerland, **5** Institute of Epidemiology I, Helmholtz Zentrum München, German Research Center for Environmental Health, Neuherberg, Germany, **6** Institute of Medical Informatics, Biometry and Epidemiology, Chair of Epidemiology, Ludwig-Maximilians-Universität, Munich, Germany, **7** Klinikum Grosshadern, Munich, Germany, **8** Functional and Adaptive Biology, Université Paris Diderot-Paris7 and CNRS, Paris, France

## Abstract

Natural variation in DNA sequence contributes to individual differences in quantitative traits. While multiple studies have shown genetic control over gene expression variation, few additional cellular traits have been investigated. Here, we investigated the natural variation of NADPH oxidase-dependent hydrogen peroxide (H<sub>2</sub>O<sub>2</sub> release), which is the joint effect of reactive oxygen species (ROS) production, superoxide metabolism and degradation, and is related to a number of human disorders. We assessed the normal variation of H<sub>2</sub>O<sub>2</sub> release in lymphoblastoid cell lines (LCL) in a family-based 3-generation cohort (CEPH-HapMap), and in 3 population-based cohorts (KORA, GenCord, HapMap). Substantial individual variation was observed, 45% of which were associated with heritability in the CEPH-HapMap cohort. We identified 2 genome-wide significant loci of Hsa12 and Hsa15 in genome-wide linkage analysis. Next, we performed genome-wide association study (GWAS) for the combined KORA-GenCord cohorts (n = 279) using enhanced marker resolution by imputation (>1.4 million SNPs). We found 5 significant associations (p < 5.00 × 10<sup>-8</sup>) and 54 suggestive associations (p < 1.00 × 10<sup>-5</sup>), one of which confirmed the linked region on Hsa15. To replicate our findings, we performed GWAS using 58 HapMap individuals and ~2.1 million SNPs. We identified 40 genome-wide significant and 302 suggestive SNPs, and confirmed genome signals on Hsa1, Hsa12, and Hsa15. Genetic loci within 900 kb from the known candidate gene p67phox on Hsa1 were identified in GWAS in both cohorts. We did not find replication of SNPs across all cohorts, but replication within the same genomic region. Finally, a highly significant decrease in H<sub>2</sub>O<sub>2</sub> release was observed in Down Syndrome (DS) individuals (p < 2.88 × 10<sup>-12</sup>). Taken together, our results show strong evidence of genetic control of H<sub>2</sub>O<sub>2</sub> in LCL of healthy and DS cohorts and suggest that cellular phenotypes, which themselves are also complex, may be used as proxies for dissection of complex disorders.

**Citation:** Attar H, Bedard K, Migliavacca E, Gagnebin M, Dupré Y, et al. (2012) Extensive Natural Variation for Cellular Hydrogen Peroxide Release Is Genetically Controlled. PLoS ONE 7(8): e43566. doi:10.1371/journal.pone.0043566

**Editor:** Sunil K. Ahuja, South Texas Veterans Health Care System and University Health Science Center San Antonio, United States of America

**Received:** September 13, 2011; **Accepted:** July 26, 2012; **Published:** August 29, 2012

**Copyright:** © 2012 Attar et al. This is an open-access article distributed under the terms of the Creative Commons Attribution License, which permits unrestricted use, distribution, and reproduction in any medium, provided the original author and source are credited.

**Funding:** The work was supported by grants from the Swiss National Science Foundation, the National Center for Competence in Research (NCCR) "Frontiers in Genetics," and the European Union FP6 "AnEUploidy" integrated project. The funders had no role in study design, data collection and analysis, decision to publish, or preparation of the manuscript.

**Competing Interests:** The authors have declared that no competing interests exist.

\* E-mail: Stylianos.Antonarakis@unige.ch (SA); homa.attar@gmail.com (HA)

#a Current address: Department of Pathology, Dalhousie University, Halifax, Canada

#b Current address: Department of Genetics and Genomic Sciences, Mount Sinai School of Medicine, New York, New York, United States of America

#c Current address: DOE Joint Genome Institute, Walnut Creek, California, United States of America

#d Current address: Molecular Genetics of Depression, Max-Planck-Institut für Psychiatrie, München, Germany

#e Current address: Functional Genomics Core, Nestle Institute of Health Sciences, Lausanne, Switzerland

## Introduction

Recent genome-wide association studies (GWAS) using clinical phenotypes have identified a large number of DNA polymorphisms that convey an increased risk for common diseases. Identified genetic loci, however, explain only a small fraction of the overall observed phenotypic variability even when assessing very large sample sizes [1–8] owing to biological complexity [9] and low penetrance of common genomic variants [10]. Small-scale

studies (<100 individuals) indicate that gene expression is genetically controlled [11–13] emphasizing the direct link between phenotypic and genotypic variation. Despite these findings, how individual genes affect disease mechanisms remains poorly understood. Working with end-members of the phenotypic spectra (gene expression or clinical phenotypes) may not be sufficient to understand disease mechanisms. To remedy some of these shortcomings, we propose to explore the genetic control of cellular phenotypes (endophenotypes) as a trait of intermediate complex-

ity. Our study will explore hydrogen peroxide ( $H_2O_2$ ) release which is associated with multiple diseases as a proxy for a complex phenotype.

Hydrogen peroxide ( $H_2O_2$ ) release is a quantitative cellular phenotype with known implications in multiple diseases [14].  $H_2O_2$  release, as measured at the extra-cellular level, includes reactive oxygen species (ROS) generation, and superoxide metabolism and degradation, all fundamental components of innate immunity. Causative associations between the phagocyte NADPH-dependent oxidase NOX complex and multiple diseases are known [14–17]. Both, low and high levels of ROS are detrimental and confer susceptibility to distinct diseases. Among these, low levels of ROS production have been shown to be associated with X-linked chronic granulomatous disease (CGD), autosomal recessive CGD, autoimmunity, and arthritis [18–23]. High ROS levels have been attributed to cardiovascular disease, hypertension, and neurodegenerative disorders [24–32]. The first evidence for genetic factors involved in ROS level regulation comes from a family-based study assessing heredity of ROS levels in essential hypertension [24]. This study found that 20–35% of the observed variation could be attributed to genetic factors. Down Syndrome (DS) individuals also show a ROS alteration suggesting that genetic loci on Homo sapiens (Hsa) chromosome 21, or loci on other chromosomes interacting with Hsa21, may be key players in ROS regulation. Despite efforts to characterize both the genetic and the molecular basis of altered ROS production in DS, insight into disease mechanisms are still lacking [33,34]. Some of the phenotypes of DS might be related to unbalanced redox-states. However, the role, impact, and consequences of low or high ROS levels in various cell types of this chromosomal abnormality remain obscure [35–39].

The major source of ROS production in lymphoblastoid cells is NOX2-dependent. NOX2-deficient lymphocytes from chronic granulomatous disease (CGD) patients produce very low levels of ROS. Expressed co-factors of NOX2 and NOX homologues in lymphoblastoid cell lines include p22<sup>phox</sup>, p47<sup>phox</sup>, p67<sup>phox</sup>, p40<sup>phox</sup>, RAC1, and RAC2. Intracellular superoxide produced by this enzyme can not diffuse through cell membranes. However, superoxide is readily converted both spontaneously and enzymatically, to hydrogen peroxide ( $H_2O_2$ ), which is membrane permeable. Superoxide dismutase (SOD), catalase, and peroxidases are associated with ROS metabolism and degradation. In this study, we measure ROS production and  $H_2O_2$  release by detecting  $H_2O_2$  release at the extra-cellular level.

The aim of this study is to evaluate the use of a cellular quantitative phenotype as a proxy to complex phenotypes by taking  $H_2O_2$  release in EBV transformed lymphoblastoid cell lines (LCL) as an example. We aim at identifying human genetic factors underlying the variability of  $H_2O_2$  release, and thus the susceptibility to infectious diseases, through a whole genome linkage and association analysis in the general healthy population. Furthermore, we evaluated levels and differences of  $H_2O_2$  release in LCL derived from Down Syndrome individuals, and identify regulatory loci which may provide insights into the biological pathways of  $H_2O_2$  variation.

## Results

### Phenotypic distribution of $H_2O_2$ release in four population-based cohorts

We observed extensive natural variation of NADPH oxidase-dependent  $H_2O_2$  release in LCL of four population-based cohorts: KORA, GenCord, HapMap, and DS (**Figure 1**). KORA is a cohort of newly established LCL derived from unrelated healthy

adults, GenCord is a cohort of newly established LCL derived from unrelated newborns, and HapMap is part of a three-generational sample cohort, from which unrelated LCL from healthy adults were used for genome wide association (GWA) analysis. A cohort of newly established LCL derived from unrelated Down Syndrome individuals were used to quantify the difference of these individuals to healthy cohorts. All cohorts are of Caucasian origin. A description of each cohort's demographic, phenotypic, and genotypic characteristics is shown in **Table 1**. We observed a mean and standard deviation for  $H_2O_2$  release (arbitrary units) of 0.51 in the KORA cohort ( $\pm 0.64$ ,  $N = 199$ ), 0.47 ( $\pm 0.38$ ,  $N = 80$ ) in GenCord, 1.22 ( $\pm 1.15$ ,  $N = 58$ ) in HapMap, and 0.23 ( $\pm 0.31$ ,  $N = 75$ ) in DS individuals (**Figure 1**, **Table 1**, **File S1**). To quantify the degree to which this observed variation was individual-specific and reproducible, we assessed phenotypes in 21 LCL of unrelated HapMap individuals in two independent experiments. We found a 28-fold inter-individual difference, and high reproducibility (ratio of coefficient of variance  $> 28$ ,  $p < 1.00 \times 10^{-4}$ , **File S2A**, Pearson correlation coefficient = 0.89,  $p < 1.00 \times 10^{-4}$ , **File S2B**). The phenotypic distribution of  $H_2O_2$  release in the DS cohort differed from all other healthy cohorts, with a significantly different distribution compared to the HapMap (Wilcoxon rank sum test,  $p < 2.88 \times 10^{-12}$ ), the GenCord ( $p < 3.11 \times 10^{-9}$ ), and the KORA cohort ( $p < 5.35 \times 10^{-9}$ , **Figure 1**).

We next aimed at identifying the genetic contribution to this natural variation in  $H_2O_2$  release. Linkage analysis was used as a first step to assess the genetic basis of  $H_2O_2$  release in the family-based HapMap-CEPH cohort, and genome-wide association analysis was conducted to refine and replicate results in the KORA, GenCord, and HapMap cohorts.

### Hydrogen peroxide release heritability and linkage analysis

We measured  $H_2O_2$  variation in human LCL from 10 CEPH-HapMap three-generation families ( $N = 113$ ). We observed extensive variation in  $H_2O_2$  release that ranged from 0.001 to 6.035 (arbitrary units). To estimate what fraction of this natural phenotypic variation could be attributed to genetic components, we performed a variance-component linkage analysis [40] and found genome-wide estimated sample heritability ( $h^2$ ) of 45%. This finding suggests that 45% of all  $H_2O_2$  release variation can be attributed to genetic factors in the cell lines used herein. In a linkage analysis of LCL of these same individuals, we identified two significant and two suggestive LOD scores on chromosomes Hsa1, Hsa12, Hsa15 and Hsa19 (**Figure 2**) with the use of 2723 SNP markers. Nominal genome-wide significance level was assessed by performing 1000 simulations in which we shuffled the phenotypes but kept the genotypes, allele frequency, and family structure constant. A LOD score of 4.48 was obtained for the nominal genome-wide significance threshold. The significant linkage signals were on Hsa12 with LOD score of 4.64 ( $p < 1.00 \times 10^{-6}$  for marker TSC0795922 at position 10,950 kb) and on Hsa15 with LOD score 4.81 ( $p < 1.00 \times 10^{-6}$  for marker TSC0181040 at position 37,068 kb). However, marker density in this linkage analysis was not sufficient to assign candidate genes. Furthermore, the linked region on Hsa12 is very gene-rich. The identified locus on Hsa15 is located 115 kb upstream of the transcription start site of MEIS2. The suggestive hit on Hsa1 had a LOD score of 4.17 ( $p < 1.00 \times 10^{-5}$ , TSC0343078 at position 4,389 kb), the second suggestive linkage signal was identified on Hsa19 with a LOD score of 3.26 ( $p < 5.00 \times 10^{-5}$ , TSC1058872 at position 54,754 kb).

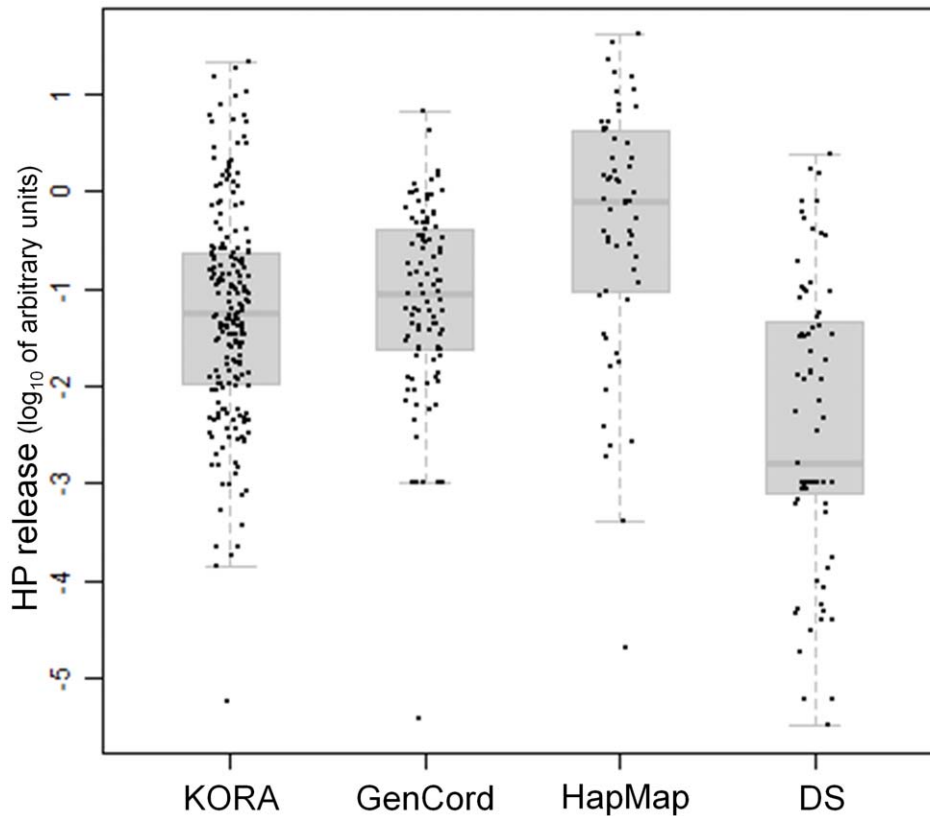


**Figure 1. Distribution of H<sub>2</sub>O<sub>2</sub> release in sample cohorts KORA, GenCord, HapMap and Down Syndrome.** Box plots (in light grey) for the sample cohorts KORA, GenCord, HapMap and Down Syndrome (DS) show the distribution of H<sub>2</sub>O<sub>2</sub> variation across cohorts. Each black dot corresponds to an individual's mean of 4 measures of H<sub>2</sub>O<sub>2</sub> release. The median is shown as a dark grey line, the low and upper end of the box plots (in light grey) indicate the first and third quartile of the distribution. The whiskers indicate the lower and upper end of the distribution. The distribution of H<sub>2</sub>O<sub>2</sub> in the Down Syndrome cohort shows a significant decrease as compared to HapMap (Wilcoxon rank sum test,  $p < 2.88 \times 10^{-12}$ ). doi:10.1371/journal.pone.0043566.g001

#### Genome-wide association analysis for KORA-GenCord

We used the KORA and GenCord cohorts as an initial combined cohort for GWA analysis and we used HapMap (N=58) as a replication cohort (see discussion). As all three cohorts were genotyped on different platforms, we obtained a common and larger set of SNPs by imputation using the HapMap Phase II genotypes as a reference (see methods, **File S3**). After applying quality filters for imputed SNPs ( $R > 0.9$ ), a total set of 1.4 out of 2.1 million SNPs was included for GWAS. We performed principal component analysis to detect outliers for each cohort separately, and excluded one sample from the GenCord cohort. Next, we assessed whether the use of multiple cohorts and imputation of SNPs did not lead to population substructure, or clustering of called versus imputed SNPs by performing both principal component analysis and multidimensional scaling for the combined three cohorts. For the PCA analysis, a random selection of 500 K SNPs, and a centered approach was used. No evident substructure was detected by visual inspection among the three cohorts (**File S4**), and by analysis of proportions of variance of components 1 to 18. The cumulative proportion of variance of the first 10 components explained only 0.039 of the observed variation (data not shown), and increased slowly with increasing components.

We found 5 significant associations ( $p < 5 \times 10^{-8}$ ) and 54 suggestive associations with p-values of less than  $1.00 \times 10^{-5}$  (**Figure 3**, **Figure 4**) with the use of a linear genetic association model and median centered phenotypic distribution (see discussion

for the choice of the design and the genetic model). These associated loci are located in 21 genetic clusters when defining a cluster as 1 mega-base of size (**Table 2** shows the top 15 clusters). Nominal unadjusted p-values from the WALD test statistics are reported. The strongest association hit was found on Hsa14 with a cluster of 7 SNPs on position 86,942 kb (top signal rs17741027,  $p = 1.23 \times 10^{-9}$ ), followed by Hsa10 with 4 SNPs at position 52,264 kb (rs16909866,  $p = 1.66 \times 10^{-8}$ ). Among these top associations ( $p < 1.00 \times 10^{-5}$ ), we could not find association on Hsa12 and Hsa15 within the genetic regions linked in the CEU-CEPH family-based cohort, but we found an overlap with a known candidate gene, p67<sup>phox</sup> (also called NOXA2 or NCF2) on Hsa1. Three SNPs are located 913 kb downstream of the candidate gene p67phox on Hsa1 (position 181,791 kb), with the strongest signal for SNP rs1535133 ( $p = 5.97 \times 10^{-7}$ , position 182,704 kb (**Figure 4**). To replicate these findings, and to investigate whether the previously linked regions were population-specific, we subsequently analyzed the population-based HapMap cohort in a GWAS.

#### Genome-wide association analysis for HapMap

We used 60 unrelated LCL of Caucasian origin from the CEPH-Hapmap cohort as a replication cohort. We determined the H<sub>2</sub>O<sub>2</sub> release in 58 samples and performed a GWAS using a total of 2,124,999 SNPs with minor allele frequency of more than 5% [41,42]. We detected highly significant association signals in this analysis (**Figure 3**, **Figure 5**). Overall, 40 SNPs reached

**Table 1.** Demographic characteristics for all four population-based cohorts.

	GENCORD	KORA	CEPH-HapMap	Down Syndrome
<b>Cohort characteristics</b>				
Origin cohort	University of Geneva, Laboratory of Prof. Antonarakis SE, Geneva, Switzerland	German Research Center for Environmental Health, Neuherberg, Germany	Coriell Cell Repositories, Camden, USA	AnEUploidy collection, Paris, France; Galliera Genetic Bank of Genoa, Italy; Emory University School of Medicine, Atlanta, USA and CSS-Mendel Institute in Rome, Italy
Origin population	Caucasian	Caucasian	Caucasian	Caucasian
Sample size	99	200	58	75
Individual's age (category)	1 day	40–60 years	>60 years	<40
Immune status	immature	mature	mature	mixed
Recently established cell line	yes	yes	no	yes
Gender (% female)	49%	56%	52%	-
<b>Phenotypic characteristics (H<sub>2</sub>O<sub>2</sub> release)</b>				
Mean	0.47	0.51	1.22	0.22
Standard deviation	±0.38	±0.64	±1.15	±0.31
Range	0.004–2.28	0.005–3.73	0.009–4.97	0.004–1.45
<b>Genotypic characteristics</b>				
Platform	Illumina 550 K	Affymetrix 6.0 500 K	multiple platforms	no genotypes
Number called SNPs	480,455	413,877	2.1 million	-
Number called and imputed SNPs	1.4 million	1.4 million	2.1 million	-

Demographic, phenotypic and genotypic characteristics for each cohort are indicated. doi:10.1371/journal.pone.0043566.t001

genome-wide significance of  $p < 5.00 \times 10^{-8}$ , and 302 suggestive SNPs of less than  $p < 1.00 \times 10^{-5}$  that correspond to 90 clusters (**Table 3** shows the top 15 clusters). The most significant loci with p-values of less than  $1.00 \times 10^{-12}$  were rs12022620 on Hsa1 (intronic SNP within *SIPA1L2*) and rs12528870 on Hsa6 (intergenic SNP, **Figure 5**). The function of *SIPA1L2* (signal-induced proliferation-associated 1 like) is not well characterized yet. Among the other strong statistical signals, we identified association signals within the genomic regions of the linked

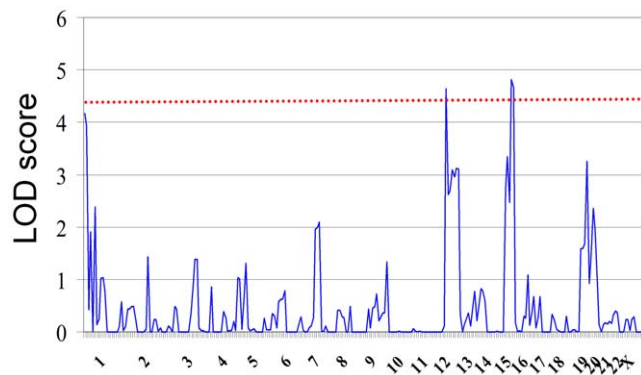


**Figure 2.** Two significant and two suggestive LOD scores on Hsa12, Hsa15, Hsa1, and Hsa19. LOD scores of genome-wide linkage analyses using the CEPH-HapMap family-cohort of three generations are plotted for all autosomal chromosomes (in blue). The blue line shows the maximal LOD score within a window size of 10 kb. The red dotted line indicates the significance level identified through 1'000 simulations. doi:10.1371/journal.pone.0043566.g002

regions. We found a cluster on Hsa12 ( $p < 1.4 \times 10^{-10}$ ) with 12 SNPs at position 4,690 kb close to *KCNA6* and *GALNT8*, and on Hsa21 (rs12483177,  $p < 1.8 \times 10^{-8}$ ) with 11 SNPs at position at 43,587 kb close to *SIK1* and *HSF2BP* (**Figure 5**). *KCNA6* (voltage-gated potassium channel) mediates the voltage-dependent potassium ion permeability of excitable membranes (UniProtKB for *KCNA6\_HUMAN*). The role of *GALNT8* (polypeptide N-acetylgalactosaminyltransferase 8) is not described in the literature. *SIK1* (salt-inducible kinase 1) has a transient role during the earliest stages of myocardial cell differentiation and/or primitive chamber formation [43] and may also be important for the earliest stages of skeletal muscle growth and/or differentiation and in G2/M cell cycle regulation [44]. In computational studies investigating Hidden Markov Chain predictions and fold recognition algorithms for kinases on HSA21, *SIK1* and three other kinases were identified to be members of a novel mitogen-activated kinase pathway (MAPK) [45].

**Comparisons across all linkage, association studies and known candidate genes**

We identified replication between the top linkage findings for four loci in the HapMap samples on Hsa1 (rs2500247 at position 3,172 kb,  $p = 4.65 \times 10^{-6}$ ), Hsa12 (rs10492058, 4,756 kb,  $p = 1.45 \times 10^{-10}$ ), and on two loci on Hsa15 (rs2075814, 22,717 kb,  $p = 4.2 \times 10^{-7}$ ; rs16947598, 43,816 kb,  $p = 1.70 \times 10^{-7}$ ). Of the known candidate genes expressed in LCL, p67<sup>phox</sup> (Hsa1, pos = 183,525 kb) overlapped with two top association signals in the KORA-GenCord GWAS and in the HapMap GWAS (KORA-GenCord, rs10489726, 913 kb downstream,  $p = 5.97 \times 10^{-7}$ ; and HapMap, rs528846, 932 kb upstream,  $p = 8.63 \times 10^{-6}$ ). We did not detect strong association findings in KORA-GenCord samples that overlapped with the

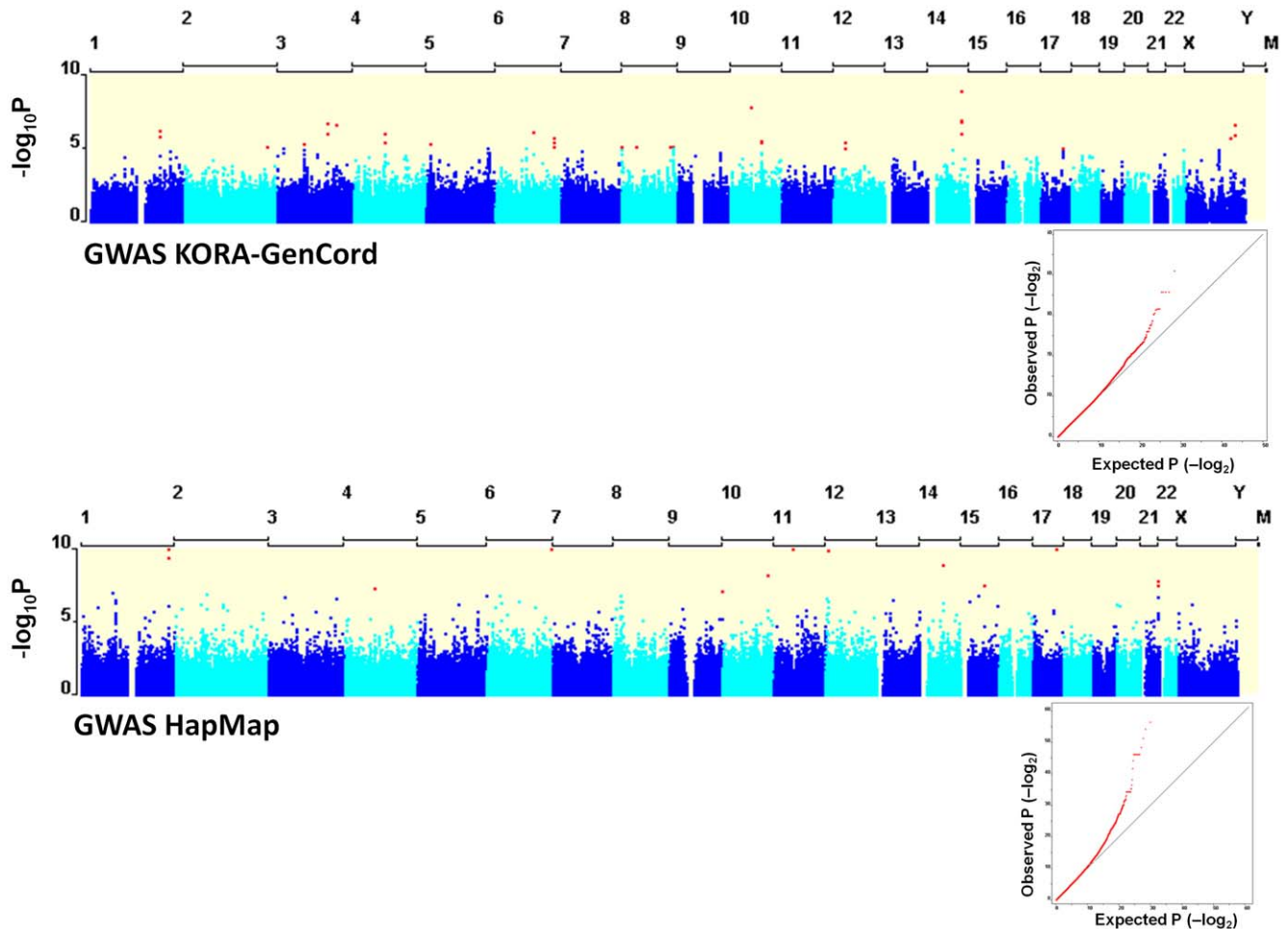


**Figure 3. Genome-wide association results for natural variation of  $H_2O_2$  release in KORA-GenCord and HapMap cohorts.** Manhattan dot plots show results for genome-wide association analysis for the KORA-GenCord and the HapMap sample cohorts. The blue dots represent the association finding of one single SNP with natural variation in  $H_2O_2$  release. Light and dark blue colors distinguish subsequent chromosomes. We did not analyze genetic markers for mitochondrial SNPs in this study. We show results of a genetic additive model indicating the unadjusted nominal  $-\log_{10}$  of p-values. Quantile plots show the observed versus the expected distribution of GWAS for both analyses. doi:10.1371/journal.pone.0043566.g003

linkage findings. Neither did we find the same replicated SNPs nor genetic regions among the two GWA studies within a distance of 1 Mb. **Table 4** indicates replicated loci among linkage and GWA.

Given the lack of replication of the top SNPs across the two GWA studies, we next asked whether we could detect enrichment of lower p-values of these top SNPs of the KORA-GenCord in the GWA HapMap. We observed an enrichment for p-values of  $p < 0.2$  in HapMap GWAS (data not shown). A similar pattern was observed when comparing top HapMap signals with p-values of all KORA-GenCord. This pattern suggests enrichment for repeated associated loci across GWAS, but this enrichment is not significant.

#### Covariate analysis

To assess the impact of potential co-variates (immune status, time of cell line establishment, individuals' age, and gender) on  $H_2O_2$  distribution, we combined all samples after median centered normalization, and estimated the relative contribution of each of the co-variates in an univariate linear regression model with a cluster effect on the population. We found that none of the covariates had a significant effect on the trait distribution. We found the following relative order of correlation: Time of

establishment of cell lines (B-coefficient = 0.142,  $p = 0.231$ ), status of immune system (B-coefficient = 0.139,  $p = 0.127$ ), individuals' age (B-coefficient = 0.109,  $p = 0.072$ ), and gender (B-coefficient = 0.052,  $p = 0.499$ ). To estimate whether a statistical model with adjustment for all co-variate was different than a model for the main variate only, we performed a randomized set of 100'000 SNPs using a multivariate linear regression model with adjustment for all co-variates and a cluster effect on the population. We compared the results of this model with an univariate model with no adjustment for co-variates. We found no significant differences between the two models for the 100'000 randomly selected SNPs. This analysis suggested that covariates did not represent a confounding factor.

#### Discussion

The most essential outcome of this study is the finding of extensive natural phenotypic variation in healthy individuals for  $H_2O_2$  release, and evidence for a genetic basis to the observed variation in LCL of the cohorts used herein. This finding is in line with several studies reporting large natural phenotypic variation, such as for gene expression level variation, many of which were

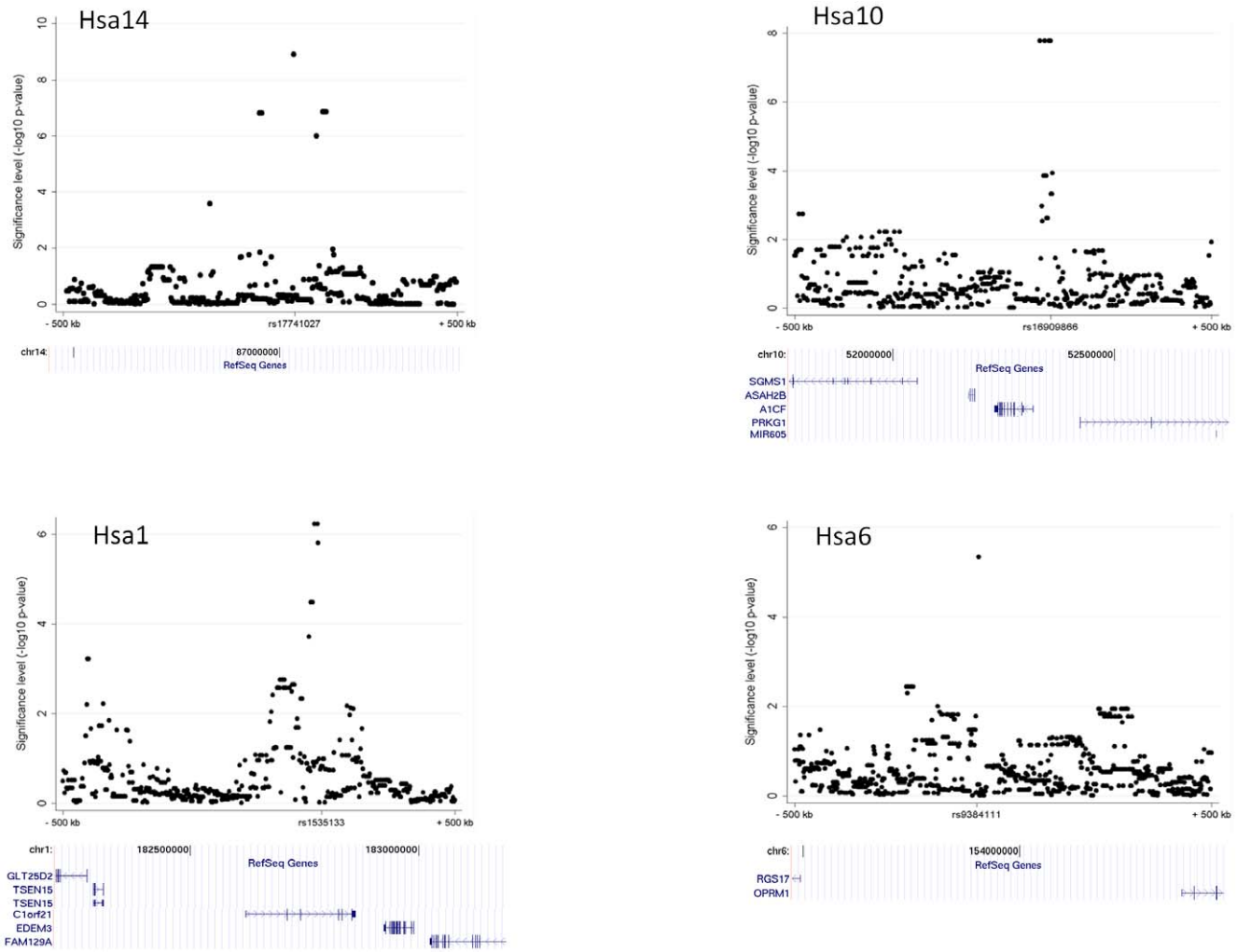


**Figure 4. Examples of significant association findings in KORA-GenCord GWA.** The significance level ( $-\log_{10} P$ ) of the top two association findings and two examples of top hits overlapping with either linkage, top GWA in HapMap, overlap with known candidate genes, or top findings on Hsa21 are shown within a genetic region of 1 Mb ( $\pm 500$  kb) around the significantly associated SNP). The chromosome, SNP ID, location and genic context (RefSeq genes, using UCSC genome browser) are indicated for each depicted SNP.  
doi:10.1371/journal.pone.0043566.g004

repeatedly shown to be shaped by genetic polymorphisms [46–50]. It may be conceivable that many traits maintain natural variation for response to selection pressure [51]. The measurements of the phenotypic spectra of  $H_2O_2$  release in more than 500 individuals in 4 healthy cohorts and in a DS cohort confirm previously reported differences in  $H_2O_2$  release of primary neutrophils of healthy individuals and individuals with chronic granulomatous disease [52], and on altered redox-states in DS individuals.

In the study of the Kuhns DB, et al., 10–20 fold differences in primary neutrophils from peripheral blood of healthy individuals were detected in comparison to individuals with chronic granulomatous disease. Also, large inter-individual differences were detected, and correlated to genotypes. This correlation was reported to be a strong predictor for overall survival of CGD patients. Our genetic study of natural variation in  $H_2O_2$  release revealed 45% of heritability, and we detected genomic regions on Hsa1, Hsa12 and Hsa15 as significant and replicated regions in more than one cohort. Results from GWAS in HapMap samples indicated an associated genetic locus close to the gene *SIK1* on Hsa21. *SIK1* is encoding a kinase known for its involvement in cardiomyogenesis by regulating cardiomyoblast cell cycle [43,44],

but it could also exert additional unknown functions. Further experiments are necessary to replicate and to assess the functional consequences of this association in DS and in healthy individuals. In our study, we did not find significant association signals on Hsa21 or any other markers close to *SIK1* in the combined KORA-GenCord GWA.

$H_2O_2$  release, an endophenotype more closely related to sequence variation (as opposed to a clinical phenotype) may be a complex trait in itself. The detection of multiple genome-wide significant loci suggests a polygenic trait. The strongest linkage results indicate loci on Hsa1, Hsa12, Hsa15 and Hsa19, two of which (Hsa1 and Hsa15) were also significantly associated in either the KORA-GenCord or HapMap GWAS, or both. However, we did not detect the same associated SNPs in the three cohorts, but replication within the same genomic regions. This may indicate either a lack of power to detect genetic loci due to the relatively small sample size, or reflect the complex genetic architecture of  $H_2O_2$  with multiple loci contributing small proportions to the observed phenotypic variation. Our study design focused on the detection of common alleles with a genetic effect of more than 5% given an allele frequency of 0.15, and with our study design, we

**Table 2.** Results from GWAS for the KORA-GenCord cohort.

SNP ID	Chr	Pos (bp)	type	Closest gene (within 1 MB)	Unadjusted p-value	Number SNPs/cluster
rs17741027	14	86941588	INTERGENIC	GALC	$1.23 \times 10^{-9}$	7
rs16909866	10	52263776	INTRONIC	ACF_HUMAN	$1.66 \times 10^{-8}$	4
rs1400014	3	132414349	INTRONIC	NEK11	$2.27 \times 10^{-7}$	2
rs3859991	X	130050216	INTRONIC	RHGXX_HUMAN	$2.64 \times 10^{-7}$	3
rs6801020	3	153876452	INTERGENIC	P2RY1	$2.68 \times 10^{-7}$	1
rs1535133	1	182704057	INTRONIC	C1orf21	$5.97 \times 10^{-7}$	3
rs9372321	6	97600416	INTRONIC	KLHL32	$8.6 \times 10^{-7}$	1
rs11728249	4	83760349	INTERGENIC	C4orf11	$1.7 \times 10^{-6}$	2
rs5909759	X	116093601	INTERGENIC	U6	$2.13 \times 10^{-6}$	3
rs9479282	6	152642425	INTRONIC	SYNE1;C6orf98	$2.23 \times 10^{-6}$	7
rs10887721	10	82035334	INTRONIC	MAT1A	$3.17 \times 10^{-6}$	2
rs4930939	12	30893752	INTERGENIC	CAPRIN2	$4.58 \times 10^{-6}$	3
rs9384111	6	153924030	INTERGENIC	U6	$4.59 \times 10^{-6}$	1
rs4701883	5	10816656	UPSTREAM	DAP	$5.43 \times 10^{-6}$	1
rs17006293	3	69777596	INTERGENIC	MITF	$5.88 \times 10^{-6}$	3

We show the results of the top 15 out of the 21 clusters of significantly associated genetic loci ( $p < 5.00 \times 10^{-8}$ ) and with suggestive associations ( $p < 1.00 \times 10^{-5}$ ) from genome-wide association analyses. We associated natural variation in  $H_2O_2$  release measured in the KORA-GenCord cohort ( $n = 279$  individuals) with more than 1.4 million markers (called and imputed SNPs). SNP ID, chromosome and position are indicated. Also, the type of SNP, the closest gene (within 1 MB), unadjusted p-value and the number of SNPs per cluster are indicated. SNP annotations were done by using the software WGAViewer (build 36, Ensembl core database *homo sapiens core 46 36h*, Ensembl variation database *homo sapiens variation 46 36h*, and Ensembl gene ontology database *ensemble go 46*). doi:10.1371/journal.pone.0043566.t002

have 80% of power to detect such a quantitative trait locus while using 300 individuals [53].

Our study design considered the use of a combined GWA of 279 individuals to increase sample size, and to replicate findings in a follow-up cohort of 58 HapMap individuals. Even though all cohorts used herein are of Caucasian origin, and population substructure did not appear to be a confounding factor, differences among these cohorts may have reduced the power to detect the same loci across cohorts. Co-variate analysis showed that the effect of the SNP on association was significant in shaping the  $H_2O_2$  trait, and suggests that despite differences in the origin of cohorts, cell line establishment and age of the cell lines the underlying genetics is the predominant factor. Further evidence for a strong genetic effect, rather than differences in cellular phenotypes in different cohorts, comes from a study by Dimas, et al. [13] showing that 83% of detected eQTLs in HapMap were replicated in GenCord samples. This finding was crucial to our study design and validates the use of the GenCord cohort as a comparable cohort to the HapMap cohort. We cannot exclude that  $H_2O_2$  release may underlie different cellular covariates than gene expression levels, leading to population-specific differences that we could not fully correct for. We investigated multiple genetic models for assessing the best method for normalization of the phenotypic distribution. We expected all cohorts to show similar distributions of  $H_2O_2$  release, as all individuals were of European ancestry, and we measured all phenotypes under standardized and highly controlled conditions. No substantial differences among cohorts could be attributed to population substructure or to known covariates. The non-normal distribution of phenotypes may probably be due to the relative small sample size, as departure from normal distribution was largest for HapMap ( $N = 58$ ) and smallest for KORA ( $N = 199$ ). As shown in Figure 1, the distribution of  $H_2O_2$  release is enriched for extreme phenotypes with individuals with either very high or very low phenotypes. To

assess the impact of the phenotypic distribution on our results, and to exclude false positive signals due to departure from model assumptions, we have considered three different methods of normalization across cohorts. Also, we compared results from parametric and non-parametric association models. We conducted log transformation, median centered and inverse variance normalization, and median centered normalization only. Log transformation did not lead to a normal distribution. When using median and inverse variance normalization we lost all association signals, leading to the hypothesis that the genetic signal may be associated with the high and low end distribution of the phenotypes. Therefore, we chose to use the median centered approach, while keeping the internal variation of each population untouched. The median centered approach does not fully support the assumption for normal distribution. To assess whether results differed due to model assumptions, we compared these results with a non-parametric regression model using the Spearman rank correlation. We found the same top association signals with both models, with the only difference of slightly lower p-values (mostly at one order of magnitude for the top signals), showing that results did not depend on model assumptions.

LCL represent a relevant physiological cell type for ROS production [14], and LCL express mainly NOX2-dependent ROS [54–56]. A study by Kobayashi, et al. [57] compared fresh neutrophils, fresh B-lymphocytes, and EBV transformed B-lymphocytes from the same individuals to compare the relative expression of NOX2. They reported that B-lymphocytes have 1.1% of the NOX2 and 2.6% of the p22 that a neutrophil has, and that this is further decreased when the cells are EBV transformed. They showed that regardless of the amount of NOX2 the neutrophil expressed, the relative expression level in a B-cell of the same individual was correlated. This study would not have been feasible without the use of immortalized cell lines for both large families and population-based collections with more than 2 million

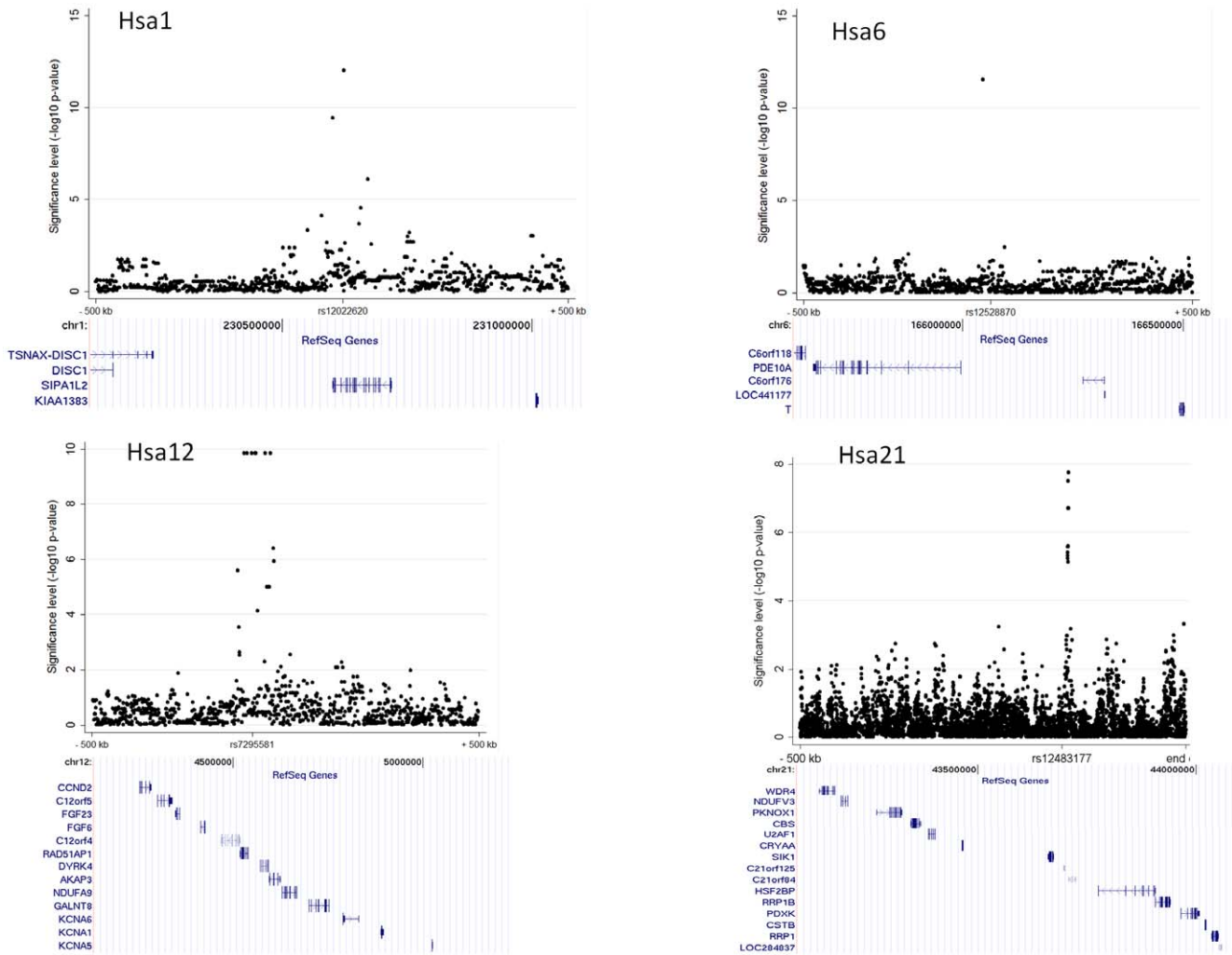


**Figure 5. Examples of significant association findings in HapMap GWA.** The significance level ( $-\log_{10} P$ ) of the top two association findings and two examples of top hits overlapping with either linkage, top GWA in KORA-GenCord, overlap with known candidate genes, or top findings on Hsa21 are shown within a genetic region of 1 Mb ( $\pm 500$  kb around the significantly associated SNP). The chromosome, SNP ID, location and genic context (RefSeq genes, using UCSC genome browser) are indicated for each depicted SNP. doi:10.1371/journal.pone.0043566.g005

genetic markers. As for all genome-wide studies using cell lines, it is a first step into identifying the genetic basis and requires validation in further cohorts, functional analysis, and ultimately verification in primary cells from healthy and diseased individuals. Potential confounding factors due to EBV-transformation remain a subject of debate and need to be considered. Also, we measured  $H_2O_2$  levels after PMA stimulation, and genetic variation involved in the *protein kinase C*, through which PMA acts directly, cannot be fully excluded. However, heritability would not have been detected if EBV transformation or PMA stimulation would affect pathways in a random way. Finally,  $H_2O_2$  release is an endophenotype with multiple levels of metabolism. Our assay relied on extracellular measures of hydrogen peroxide release which is the joint result of ROS production, metabolism, and degradation. Each step of these mechanisms may involve few or many genes, and thus contribute to the complexity of the phenotype.

We did not find genome-wide significant associations for loci of the NADPH-dependent NOX2 and other NOX related genes. We identified a locus 1 Mb from p67<sup>phox</sup> (or NCF2) as the closest hit for NOX2 members expressed in LCL (p22<sup>phox</sup>, p40<sup>phox</sup>, p47<sup>phox</sup>, p67<sup>phox</sup>, and homologues RAC1 and RAC2). These results suggest

that variation in other genetic loci have stronger impact on natural variation of  $H_2O_2$  as compared to the known genes identified in studies of Mendelian disorders. Previous case-control studies investigating the molecular basis of either  $H_2O_2$  or ROS applied candidate gene approaches with contradictory results. Some studies identified mutations or polymorphisms associated with ROS generation within the NADPH-dependent NOX2 gene or its cofactors, while others found no association [31]. Recently, it has been suggested that haplotype rather than single SNP analysis may capture more of the relevant biological effects of phenotypic traits. Indeed, in the case of NOX2 dependent ROS generation, Bedard and coworkers [16] report an association between p22<sup>phox</sup> (also called *CYBA*) haplotypes, rather than single polymorphisms. The associated haplotype was shown to act, at least in part, through an effect on protein expression levels. While this approach shed some light on the contradictory results reported so far on the involvement of NADPH-dependent NOX components in ROS generation, the large observed natural variation could not solely be attributed to the NADPH-dependent NOX2 and its cofactors, leading to the hypothesis that other loci are involved in regulatory mechanisms.

**Table 3.** Results from GWAS for the HapMap cohort.

SNP ID	Chr	Pos (bp)	type	Closest gene (within 1 MB)	Unadjusted p-value	Number SNPs/cluster
rs12022620	1	230616732	INTRONIC	SIPA1L2	1.00×10 <sup>-12</sup>	3
rs12528870	6	166117266	INTERGENIC	U6	3.00×10 <sup>-12</sup>	1
rs12602262	17	62290605	INTERGENIC	CACNG5	1.20×10 <sup>-11</sup>	1
rs11039359	11	47704385	INTRONIC	FBNP4	4.80×10 <sup>-11</sup>	1
rs7295581	12	4690362	INTERGENIC	GALNT8	1.45×10 <sup>-10</sup>	12
rs17833323	14	58415000	INTERGENIC	DACT1	1.32×10 <sup>-9</sup>	32
rs10749212	10	118166653	INTERGENIC	PNLIPRP3	7.27×10 <sup>-9</sup>	7
rs12483177	21	43586879	INTERGENIC	Q6ZN03_HUMAN	1.75×10 <sup>-8</sup>	13
rs6494367	15	61002704	INTERGENIC	TLN2	3.6×10 <sup>-8</sup>	1
rs17001416	4	77250823	INTRONIC	ART3	4.84×10 <sup>-8</sup>	20
rs2297721	9	138776337	INTRONIC	NP_976222.1	8.64×10 <sup>-8</sup>	3
rs17005290	2	81322921	INTERGENIC	5S_rRNA	1.45×10 <sup>-7</sup>	3
rs466886	6	33348677	INTRONIC	RPS18	1.67×10 <sup>-7</sup>	1
rs16947598	15	43815915	INTERGENIC	SQRDL	1.70×10 <sup>-7</sup>	1
rs333036	8	19026645	INTERGENIC	PSD3	1.76×10 <sup>-7</sup>	11

Results show the top 15 out of the 90 clusters of significantly associated genetic loci ( $p < 5.00 \times 10^{-8}$ ) and with suggestive associations ( $p < 1.00 \times 10^{-5}$ ) from genome-wide association analyses. We associated natural variation in H<sub>2</sub>O<sub>2</sub> release measured in the HapMap cohort (n = 58 individuals) with more than 2.2 million markers. SNP ID, chromosome and position are indicated. Also, the type of SNP, the closest gene (within 1 MB), the unadjusted p-value and the number of SNP per cluster are indicated. SNP annotations were done by using the software WGAViewer (build 36, Ensembl core database *homo sapiens core 46 36h*, Ensembl variation database *homo sapiens variation 46 36h*, and Ensembl gene ontology database *ensemble go 46*). doi:10.1371/journal.pone.0043566.t003

Taken together, our results indicate that there is a substantially large contribution of genetic factors at the basis of H<sub>2</sub>O<sub>2</sub> release among healthy individuals in the cohorts used in this study. Our results suggest that this trait, even though an endophenotype, is

complex and that multiple genes or regulatory elements are probably acting in concert to shape its expression. The herein identified association findings, together with the closeby genes may be enriched for biologically significant genes, and/or genetic loci

**Table 4.** Overlap between top hits from linkage and GWAS.

Results for linkage and overlap with GWAS	Hsa1	Hsa12	Hsa15	Hsa19
<b>Linkage results (LOD&gt;3)</b>	<b>TSC0774051 - TSC0393286</b>	<b>TSC0795922 - TSC0431222</b>	<b>TSC0453546 - TSC1202583</b>	<b>TSC1058872 -TSC0057999</b>
	1,864 kb–7'905 kb	10,841–13'493 kb	21,775–21'897 kb	59,446–59,469 kb
	LOD = 4.17	LOD = 4.64	LOD = 3.34	LOD = 3.26
		<b>TSC0796032-TSC0014204</b>	<b>TSC0181040-TSC0940969</b>	
		54,428–54,474 kb	34,855–37,771 kb	
		LOD = 3.09	LOD = 4.81	
		<b>TSC0209972-TSC0621539</b>	<b>TSC0577078</b>	
		96,905–99,714 kb	43,404 kb	
		LOD = 3.12	LOD = 4.4	
<b>KORA-GenCord (top associations) - overlap with linkage</b>	-	-	-	-
<b>HapMap (top associations) overlap with linkage</b>	<b>rs2500247</b>	<b>rs10492058</b>	<b>rs2075814</b>	-
	3,172 kb	4,756 kb	22,717 kb	
	p = 4.65×10 <sup>-6</sup>	p = 1.45×10 <sup>-10</sup>	p = 4.2×10 <sup>-7</sup>	
			<b>rs16947598</b>	
			43,816 kb	
			p = 1.70×10 <sup>-7</sup>	

This table indicates replicated genetic regions identified through GWA in KORA-GenCord and in HapMap. Top hits for GWAS are shown when the loci overlap within 5 Mb of distance from top linkage hits. The chromosome, the genetic marker, the position and the LOD score or the p-value is shown. doi:10.1371/journal.pone.0043566.t004

relevant to pathogen defense and signaling, and pathway analysis may constitute the next step into the understanding of the regulation of H<sub>2</sub>O<sub>2</sub> release. More generally, the elucidation of the genetic control of some heritable cellular traits may also be a complex problem that requires combined approaches and extensive sample sizes.

## Materials and Methods

### Sample collections and genotyping

**CEPH\_HapMap sample collection:** We acquired EBV-transformed lymphoblastoid cell lines (beta-LCL) of 10 families (1333, 1334, 1340, 1341, 1345, 1346, 1347, 1362, 1408, 13292) and of 60 unrelated individuals of Caucasian origin from the Coriell Cell Repositories (Coriell Cell Services, Coriell Institute for Medical Research, Camden, NJ, USA; <http://ccr.coriell.org>). These are considered as healthy individuals and form part of the Caucasians of European Ancestry (CEPH) and the Haplotype Map (HapMap) Project [41,42]. Genotypes of the 10 families were downloaded from the CEPH database [50]. A total of 2723 single nucleotide polymorphisms (SNPs) were used for subsequent linkage analyses. For the 60 unrelated individuals, we used 2'124'999 million SNPs from publicly available databases, and from HapMart, NCBI\_Build36 ([http://snp.cshl.org/linkage\\_maps](http://snp.cshl.org/linkage_maps); [www.hapmap.org](http://www.hapmap.org); [41,42]).

**KORA sample collection:** KORA S4 (Cooperative Health Research in the Augsburg Region) is a sample collection of a population-based project conducted from 1999–2001 for which beta-LCL of healthy adults from the Augsburg region in Germany were established [58]. Two hundred LCL from this collection were used; these samples were genotyped with the Affymetrix 500 K oligonucleotide array containing a total of 500,568 SNPs (Affymetrix 6.0 chips). Genotypes were determined using the software BRLMM version 1.4.0 with standard settings proposed by the manufacturer. A total of 413,877 SNPs passed quality control filters and were used for further analysis.

**GenCord sample collection:** The GenCord (Geneva Cord sample collection, University of Geneva, Medical School, Geneva, Switzerland) sample collection is a population-based collection of LCL derived from umbilical cords of 200 healthy newborns of Western European origin. The sample collection was approved by the institutional ethics committee, and all mothers provided their informed consent prior to sample collection [13]. There are no phenotypic data on these newborns. DNA samples were extracted from cord tissue LCL with the Puregene cell kit (Gentra-Qiagen, Venlo, The Netherlands). Genotyping was performed with the illumina 550 K SNP (Illumina, San Diego, CA) array following the instructions of the manufacturers. From a total of 555,352 SNPs, 480,455 SNPs passed quality filters and were used for subsequent analysis.

Filter settings for genotype quality required accuracy of sample call rates of more than 98% were (estimated based on 5 duplicated genotyping of samples). Any SNP with a call rate of less than 99% call rate was excluded, as well as all SNPs called less than in 1% of all samples. Separation of homozygote and heterozygote SNPs was verified and corrected if needed (cluster separation >0.3 was required). The range of excess of heterozygosity was verified and SNPs not falling into the range of -0.1 to -1, and 0.1 to 1 were excluded. MAF was set to >5%; to exclude samples with cryptic relatedness, IBD was set to >0.125; and deviation of Hardy Weinberg equilibrium was defined as <0.05. We verified the specified gender, and visualized a random set of 100 SNPs for quality checking.

**Down syndrome sample collection:** 33 Down syndrome (DS) LCL samples were acquired from the Galliera Genetic Bank of Genoa, Emory University School of Medicine in Atlanta, and CSS-Mendel Institute in Rome [59] and 42 LCL from the AnEUploidy collection in Paris, France. Full trisomy was assessed by karyotyping. We excluded potential clustering effects of H<sub>2</sub>O<sub>2</sub> release due to the multiple origins of these samples, no substructure was detected.

**Cell culture:** The LCL of all three populations were cultured in RPMI 1640 with Glutamax I medium (Invitrogen) supplemented with 10% fetal calf serum and 1% mix of penicillin, fungizone, and streptomycin (Invitrogen). All cell lines were grown and maintained for at least 2 weeks at a constant density of 200–400,000 cells/ml. Cells were washed once with PBS (Invitrogen) to reduce accumulation of cell debris 4–5 days prior to measuring ROS production.

**AmplexRed ROS measurements:** Cell lines were assessed for H<sub>2</sub>O<sub>2</sub> release using AmplexRed (Invitrogen), a quantitative enzymatic assay that detects H<sub>2</sub>O<sub>2</sub> in the culture media. Ninety minutes prior to AmplexRed measurements, cell lines were centrifuged at 1000 rpm for 10 min and transferred to 2.5 ml Hanks' balanced salt solution (HBSS) media (containing 5% of glucose) and kept on ice. 0.5 ml of each cell line was used for measuring cell number by Fluorescent Activated Cell Sorting (FACS). Beads were added at a known concentration to obtain absolute values of cell number. Cells were diluted to a final concentration of 500,000 cells/ml.

AmplexRed measurements were performed according to manufacturers' instructions with minor modifications. In brief, 50,000 cells were plated in 0.2 ml volume of HBSS containing 25 mM AmplexRed and 0.005 U/ml horseradish peroxidase. NADPH oxidase activity was stimulated with 0.1 mM phorbol 12-myristate 13-acetate (PMA). In 1 of 5 replicates per individual cell line, 10 mM diphenyleneiodonium (DPI), an NADPH oxidase inhibitor [60], was added prior to stimulation. Fluorescence was recorded every minute for a minimum of 30 min with excitation and emission wavelengths of 550 nm and 600 nm, respectively in a BMG Fluostar microplate reader at 37°C.

**Experimental design and normalization of H<sub>2</sub>O<sub>2</sub>:** Each well-plate was set up with 12 individual cell lines. Each cell line was measured in 4 replicates in addition to one replicate that was inhibited with DPI. From the 4 replicates per sample, one was removed based on an outlier detection procedure, and the average of the remaining 3 replicates was used as the phenotypic read-out. We defined the phenotypic read-out as the maximal slope over 5 time points within 30 min of measurements. The standard curve of H<sub>2</sub>O<sub>2</sub> was used to transform relative H<sub>2</sub>O<sub>2</sub> measures to absolute values for each individual plate, thus allowing for comparison among different plates. Experiments for which regression of the standard curve of H<sub>2</sub>O<sub>2</sub> did not reach R<sup>2</sup> of 0.99 were excluded. For normalization across plates, the same 2 individuals (GM0755 and GM07341) were measured on every plate and served as a reference for normalization. As a negative control cell line, an LCL of a patient with chronic granulomatous disease (CGD) was tested to ensure specificity of the assay for NOX2-dependent H<sub>2</sub>O<sub>2</sub> detection.

### Statistical analysis

**Linkage analysis and heritability estimate:** Heritability analysis was performed with MERLIN software [40]. We assessed 113 individuals and their corresponding ROS production from 10 CEPH-HapMap families. Genetic markers for 2723 SNPs from the CEPH database ([http://snp.cshl.org/linkage\\_maps](http://snp.cshl.org/linkage_maps)); [61] were

used. Mendelian inconsistencies and unlikely genotypes were removed using PEDCHECK and PEDWIPE software [62,40].

For genome-wide linkage analysis, the same phenotypes and genotypes were used for multipoint variance component analysis [40]. Empirical significance of the linkage results were obtained from 1000 simulations by randomly redistributing the phenotypes and recalculating the maximal linkage signal genome-wide. We extracted the lowest p-value from each simulation to obtain a null distribution. Observed and expected p-values were compared to assess the nominal genome-wide significance threshold. All simulations were performed using R on a cluster of 32 HP/Intel Itanium 2 based servers at the Vital-IT Center, Lausanne, Switzerland (<http://www.vital-it.ch>). Mapping positions of these markers correspond to NCBI36/hg18.

**Normalization of phenotypes across populations:** We applied a median centered transformation for the phenotypes before combining the data from KORA and GenCord populations. HapMap samples were used as a replication cohort and were analyzed separately; and also analyzed with a median centered transformation.

**Association studies:** Imputation of SNPs across all 3 populations. We imputed SNPs from unphased alleles for 337 individuals by using the BEAGLE 3.0.4 software [63]. The HapMap sample collection with 2.2 million SNPs was used as the reference to impute SNPs for the KORA and GenCord collections. All SNPs were mapped to the same strand as the reference and A/T, C/G SNPs were discarded, resulting in 456,122, and 311,949 SNPs for KORA and GenCord, respectively. We set a threshold for the inclusion of an imputed SNP at allelic  $R^2 > 0.9$  to ensure high quality imputation. Of all 2.2 million imputed SNPs, 1.4 million were retained for further analyses.

**Principal component analysis:** Principal component analysis was first performed for samples of each cohort, and we excluded one sample from the GenCord population after visual inspection of the first 10 components. Principal component analysis of a random set of 500,000 SNPs was then used to test for population substructure among all three cohorts. Visual inspection of the first to the 8<sup>th</sup> component did not reveal evidence for substantial population substructures.

**Genome-wide association studies:** We performed linear regression analyses and an additive genetic model to perform association between  $H_2O_2$  levels and each SNP using PLINK software [64]. SNPs were coded 0, 1, or 2 for homozygous rare, heterozygous, and homozygous common alleles, respectively. For this additive model, we fitted a linear regression of the form

$$Y_i = b_0 + b_1 X_i + \varepsilon_i$$

We report the nominal  $p$ -value of the test of no association, i.e.,  $b_1 = 0$  where  $Y_i$  are the  $H_2O_2$  release for each sample  $i$ ,  $X_i$  are the genotypes coded as 0,1,2 and  $\varepsilon_i$  are assumed to be independent normally distributed random errors with mean 0 and constant variance. Mapping positions of GWA markers for KORA/GenCord and for HapMap correspond to NCBI36/hg18.

**Covariate analysis:** We combined all samples from HapMap, KORA and GenCord after median transformation of the  $H_2O_2$  release phenotype ( $N = 337$ ). The following covariates were assigned to each individual: The status of the immune system of the individual (“mature” for HapMap and KORA, “immature” for GenCord); gender; the time of cell lines establishment prior to use in this study (“old” for HapMap, “new” for KORA and GenCord); the age of the individual (“>60 years” for HapMap, “40–60 years”

for KORA, “1 day” GenCord). A clustering effect was set for each of the three populations. We conducted a general linear mixed effect regression model with a clustering effect for the population and adjustment for immune status, gender, cell line age, and individual age. We performed univariate mixed effect linear regression with a cluster effect on populations for each co-variate. We then used a multivariate mixed effect linear regression with adjustment for all co-variables and a cluster effect on populations for a randomized set of 100’000 SNPs. This model was compared to a univariate mixed effect linear regression using the SNP only.

## Supporting Information

### File S1 Sample collection identifiers and phenotypes.

All individuals used in this study are indicated with their identifier and their phenotype.  $H_2O_2$  release indicates normalized hydrogen peroxide release levels, units are arbitrary. (DOC)

### File S2 Extensive inter-individual variation and high reproducibility for $H_2O_2$ phenotypes.

(A)  $H_2O_2$  release for 21 CEPH-HapMap unrelated individuals, each of which was measured in 4 replicates is shown. Each bar corresponds to the normalized  $H_2O_2$  release of an individual, and standard deviations of three replicates per individual are indicated in red. The coefficient of variance is  $>28$  with a p-value of  $p < 1.00 \times 10^{-4}$ , indicating that there is 28 times more variation among individuals than among replicates. (B)  $H_2O_2$  release for the same 21 individuals was measured several weeks later, to estimate the reproducibility of the phenotype. Comparison for individuals of both experimental sets indicates a coefficient of correlation of more than 0.89 (Pearson correlation test,  $p < 1.00 \times 10^{-4}$ ). (TIF)

### File S3 Overlap of SNPs among the three sample cohorts and genotyping platforms.

This schematic figure displays the number of individuals genotyped for each cohort, and the number of SNPs genotyped per population. The overlap between the circles shows the numbers and percentages of overlapping SNPs among populations and genotyping platforms. (TIF)

### File S4 Principal component analysis indicates no apparent substructure.

A random set of 500,000 SNPs of 337 individuals from three cohorts was analyzed using centered principal component analysis (PCA). Here we show PC1 versus PC2. No evident substructure is apparent among cohorts. (PNG)

## Acknowledgments

We thank Lena Serrander and Laetitia Fioraso-Cartier for assistance with establishing the  $H_2O_2$  assay, and Josiane Wyniger for technical assistance in genotyping. We thank Bernd Kranz for providing cell lines for KORA, and Clementine Ripoll for technical assistance in cell line processing for the Down Syndrome cohort. Denis Cohen assisted in data managing, and Rosemary Sudan helped editing the manuscript.

## Author Contributions

Advised on study design and analysis: SEA KHK ETD. Conceived and designed the experiments: HA SEA KB KHK. Performed the experiments: HA KB. Analyzed the data: HA EM KB. Contributed reagents/materials/analysis tools: SEA KHK EW HP TM JMD MG YD PD CB SD DM. Wrote the paper: HA SEA.

## References

- Hindorf LA, Sethupathy P, Junkins HA, Ramos EM, Mehta JP, et al. (2009) Potential etiologic and functional implications of genome-wide association loci for human diseases and traits. *Proc Natl Acad Sci U S A*. Jun 9;106(23):9362–7.
- Risch NJ and Merikangas K (1996) The future of genetic studies of complex human diseases. *Science*. 273, pp. 1516–1517.
- Risch NJ (2000) Searching for genetic determinants in the new millennium. *Nature*. 405, pp. 847–856.
- McCarthy MI, Abecasis GR, Cardon LR, Goldstein DB, Little J, et al. (2008) Genome-wide association studies for complex traits: consensus, uncertainty and challenges. *Nat Rev Genet*. May;9(5):356–69.
- McCarthy MI, Hirschhorn JN (2008) Genome-wide association studies: potential next steps on a genetic journey. *Hum Mol Genet*. Oct 15;17(R2):R156–65.
- Altshuler D, Daly MJ, Lander ES (2008) Genetic mapping in human disease. *Science*. Nov 7;322(5903):881–8.
- Visscher PM, Hill WG, Wray NR (2008) Heritability in the genomics era—concepts and misconceptions. *Nat Rev Genet*. Apr;9(4):255–66.
- Manolio TA, Collins FS, Cox NJ, Goldstein DB, Hindorf LA, et al. (2009) Finding the missing heritability of complex diseases. *Nature*. Oct 8;461(7265):747–53.
- Carlson CS, Eberle MA, Kruglyak L, Nickerson DA (2004) Mapping complex disease loci in whole-genome association studies. *Nature*. May 27;429(6990):446–52.
- Antonarakis SE, Chakravarti A, Cohen JC, Hardy J (2010) Mendelian disorders and multifactorial traits: the big divide or one for all? *Nat Rev Genet*. May;11(5):380–4.
- Stranger BE, Forrest MS, Clark AG, Minichiello MJ, Deutsch S, et al. (2005) Genome-wide associations of gene expression variation in humans. *PLoS Genet*. Dec;1(6).
- Dermitzakis ET, Clark AG (2009) Genetics. Life after GWA studies. *Science*. Oct 9;326(5950):239–40.
- Dimas AS, Deutsch S, Stranger BE, Montgomery SB, Borel C, et al. (2009) Common regulatory variation impacts gene expression in a cell type-dependent manner. *Science*. Sep 4;325(5945):1246–50.
- Bedard K, Krause KH (2007) The NOX family of ROS-generating NADPH oxidases. *Physiol Reviews*. 87: 245–313, 2007.
- Holland SM (2010) Chronic granulomatous disease. *Clin Rev Allergy Immunol*. Feb;38(1):3–10.
- Bedard K, Attar H, Bonnefont J, Jaquet V, Borel C, et al. (2009) Three common polymorphisms in the CYBA gene form a haplotype associated with decreased ROS generation. *Hum Mutat*. Jul;30(7):1123–33.
- Piirila H, Valiaho J, Vihinen M (2006) Immunodeficiency mutation databases (IDbases). *Hum Mutat*. 27:1200–8.
- Dinauer MC, Curnutte JT, Rosen H, Orkin SH (1989) A missense mutation in the neutrophil cytochrome b heavy chain in cytochrome-positive X-linked chronic granulomatous disease. *J Clin Invest*. Dec;84(6):2012–6.
- Dinauer MC, Pierce EA, Erickson RW, Muhlebach TJ, Messner, et al. (1991) Point mutation in the cytoplasmic domain of the neutrophil p22-phox cytochrome b subunit is associated with a nonfunctional NADPH oxidase and chronic granulomatous disease. *Proc Natl Acad Sci U S A*. Dec 15;88(24):11231–5.
- Noack D, Rae J, Cross AR, Muñoz J, Salmen S, et al. (1999) Autosomal recessive chronic granulomatous disease caused by novel mutations in NCF-2, the gene encoding the p67-phox component of phagocyte NADPH oxidase. *Hum Genet*. Nov;105(5):460–7.
- Olofsson P, Holmberg J, Tordsson J, Lu S, Akerström B, et al. (2003) Positional identification of Ncf1 as a gene that regulates arthritis severity in rats. *Nat Genet*. Jan;33(1):25–32.
- Hultqvist M, Bäcklund J, Bauer K, Gelderman KA, Holmdahl R (2007) Lack of reactive oxygen species breaks T cell tolerance to collagen type II and allows development of arthritis in mice. *J Immunol*. Aug 1;179(3):1431–7.
- Hultqvist M, Olofsson P, Holmberg J, Bäckström BT, Tordsson J, et al. (2004) Enhanced autoimmunity, arthritis, and encephalomyelitis in mice with a reduced oxidative burst due to a mutation in the Ncf1 gene. *Proc Natl Acad Sci U S A*. Aug 24;101(34):12646–51.
- Lacy F, Kailasam MT, O'Connor DT, Schmid-Schonbein GW, Parmer RJ (2000) Plasma hydrogen peroxide production in human essential hypertension: role of heredity, gender, and ethnicity. *Hypertension*. 36:878–84.
- Dominiczak AF, Brain N, Charchar F, McBride M, Hanlon N, et al. (2004) Genetics of hypertension: lessons learnt from mendelian and polygenic syndromes. *Clin Exp Hypertens*. Oct–Nov;26(7–8):611–20.
- Mein CA, Caulfield MJ, Dobson RJ, Munroe PB (2004) Genetics of essential hypertension. *Hum Mol Genet*. Apr 1;13 Spec No 1:R169–75.
- Del Campo M, Antonell A, Magano LF, Muñoz EJ, Flores R, et al. (2006) Hemizyosity at the NCF1 gene in patients with Williams-Beuren syndrome decreases their risk of hypertension. *Am J Hum Genet*. Apr;78(4):533–42.
- Moreno MU, San José G, Fortuño A, Beloqui O, Diez J, et al. (2006) The C242T CYBA polymorphism of NADPH oxidase is associated with essential hypertension. *J Hypertens*. Jul;24(7):1299–306.
- Deng AY (2007) Genetic basis of polygenic hypertension. *Hum Mol Genet*. Oct 15;16 Spec No. 2:R195–202.
- Krause KH (2007) Aging: a revisited theory based on free radicals generated by NOX family NADPH oxidases. *Exp Gerontol*. 42:256–62.
- San Jose G, Fortuno A, Beloqui O, Diez J, Zalba G (2008) NADPH oxidase CYBA polymorphisms, oxidative stress and cardiovascular diseases. *Clin Sci (Lond)*. 114:173–82.
- Arca M, Conti B, Montali A, Pignatelli P, Campagna F, et al. (2008) C242T polymorphism of NADPH oxidase p22phox and recurrence of cardiovascular events in coronary artery disease. *Arterioscler Thromb Vasc Biol*. 28:752–7.
- Antonarakis SE, Lyle R, Dermitzakis ET, Raymond A, Deutsch S (2004) Chromosome 21 and down syndrome: from genomics to pathophysiology. *Nat Rev Genet*. Oct;5(10):725–38.
- Antonarakis SE, Epstein CJ (2006) The challenge of Down syndrome. *Trends Mol Med*. Oct;12(10):473–9.
- Kedziora J, Bartosz G (1988) Down's syndrome: a pathology involving the lack of balance of reactive oxygen species. *Free Radic Biol Med*. 4(5):317–30.
- Elroy-Stein O, Groner Y (1988) Impaired neurotransmitter uptake in PC12 cells overexpressing human Cu/Zn-superoxide dismutase. Implication for gene dosage effects in Down syndrome. *Cell*. 52 pp. 259–267.
- Busciglio J, Pelsman A, Wong C, Pigo G, Yuan M, et al. (2002) Altered metabolism of the amyloid-precursor protein is associated with mitochondrial dysfunction in Down's syndrome. *Neuron*. 33(5):677–88.
- Busciglio J, Yankner BA (1995) Apoptosis and increased generation of reactive oxygen species in Down's syndrome neurons in vitro. *Nature*. Dec 21–28;378(6559):776–9.
- Helguera P, Pelsman A, Pigo G, Wolvetang E, Head E (2005) ets-2 promotes the activation of a mitochondrial death pathway in Down's syndrome neurons. *J Neurosci*. 25(9):2295–303.
- Abecasis GR, Cherny SS, Cookson WO, Cardon LR (2002) Merlin—rapid analysis of dense genetic maps using sparse gene flow trees. *Nat Genet*. Jan;30(1):97–101.
- The International HapMap Consortium (2005) A Haplotype Map of the Human Genome. *Nature*. Oct 27;437(7063):1299–320.
- International HapMap Consortium, Frazer KA, Ballinger DG, Cox DR, Hinds DA, et al. (2007) A second generation human haplotype map of over 3.1 million SNPs. *Nature*. Oct 18;449(7164):851–61.
- Romito A, Lonardo E, Roma G, Minchiotti G, Ballabio A, et al. (2010) Lack of sik1 in mouse embryonic stem cells impairs cardiomyogenesis by down-regulating the cyclin-dependent kinase inhibitor p57kip2. *PLoS One*. Feb 3;5(2):e9029.
- Stephenson A, Huang GY, Nguyen NT, Reuter S, McBride JL, et al. (2004) snflk encodes a protein kinase that may function in cell cycle regulation. *Genomics*. Jun;83(6):1105–15.
- Pellegrini-Calace M, Tramontano A (2006) Identification of a novel putative mitogen-activated kinase cascade on human chromosome 21 by computational approaches. *Bioinformatics*. Apr 1;22(7):775–8.
- Cheung VG, Conlin LK, Weber TM, Arcaro M, Jen KY, et al. (2003) Natural variation in human gene expression assessed in lymphoblastoid cells. *Nat Genet*. Mar;33(3):422–5.
- Schadt EE, Monks SA, Drake TA, Lusk AJ, Che N, et al. (2003) Genetics of gene expression surveyed in maize, mouse and man. *Nature*. 422:297–302.
- Monks SA, Leonardson A, Zhu H, Cundiff P, Pietrusiak P, et al. (2004) Genetic Inheritance of Gene Expression in Human Cell Lines. *Am J Hum Genet*. 75(6):1094–105.
- Morley M, Molony CM, Weber TM, Devlin JL, Ewens KG, et al. (2004) Genetic analysis of genome-wide variation in human gene expression. *Nature*. 12;430(7001):743–7.
- Spielman RS, Bastone LA, Burdick JT, Morley M, Ewens WJ, et al. (2007) Common genetic variants account for differences in gene expression among ethnic groups. *Nat Genet*. 39(2):226–31.
- Stearns SC, Byars SG, Govindaraju DR, Ewbank D (2010) Measuring selection in contemporary human populations. *Nat Rev Genet*. 2010 Sep;11(9):611–22.
- Kuhns DB, Alvord WG, Heller T, Feld JJ, Pike KM, et al. (2010) Residual NADPH oxidase and survival in chronic granulomatous disease. *N Engl J Med*. Dec 30;363(27):2600–10.
- Purcell S, Cherny SS, Sham PC (2003) Genetic Power Calculator: design of linkage and association genetic mapping studies of complex traits. *Bioinformatics*. Jan;19(1):149–50.
- Piccoli C, Ria R, Scrima R, Cela O, D'Aprile A, et al. (2005) Characterization of mitochondrial and extra-mitochondrial oxygen consuming reactions in human hematopoietic stem cells. Novel evidence of the occurrence of NAD(P)H oxidase activity. *J Biol Chem*. 280: 26467–26476.
- Gruhne B, Sompallae R, Marescotti D, Kamranvar SA, Gastaldello S, et al. (2009) The Epstein-Barr virus nuclear antigen-1 promotes genomic instability via induction of reactive oxygen species. *Proc Natl Acad Sci U S A*. Feb 17;106(7):2313–8.
- Winterbourn CC (2008) Reconciling the chemistry and biology of reactive oxygen species. *Nat Chem Biol*. May;4(5):278–86.
- Kobayashi S, Imajoh-Ohmi S, Kuribayashi F, Nunoi H, Nakamura M, et al. (1995). Characterization of the superoxide-generating system in human peripheral lymphocytes and lymphoid cell lines. *J Biochem*. 1995 Apr;117(4):758–65.

58. Wichmann HE, Gieger C, Illig T (2005) KORA-gene-resource for population genetics, controls and a broad spectrum of disease phenotypes. *Gesundheitswesen*. 67(Suppl 1):S26–30.
59. Prandini P, Deutsch S, Lyle R, Gagnebin M, Delucinge Vivier C, et al. (2007) Natural gene-expression variation in Down syndrome modulates the outcome of gene-dosage imbalance. *Am J Hum Genet*. Aug;81(2):252–63.
60. Hancock JT, Jones OT (1987) The inhibition by diphenyleioidonium and its analogues of superoxide generation by macrophages. *Biochem J*. Feb 15;242(1):103–7.
61. Matise TC, Sachidanandam R, Clark AG, Kruglyak L, Wijsman E, et al. (2003) A 3.9-centimorgan-resolution human single-nucleotide polymorphism linkage map and screening set. *Am J Hum Genet*. Aug;73(2):271–84.
62. O'Connell JR, Weeks DE (1998) PedCheck: a program for identification of genotype incompatibilities in linkage analysis. *Am J Hum Genet*. Jul;63(1):259–66.
63. Browning BL, Browning SR (2011) A fast, powerful method for detecting identity by descent. *Am J Hum Genet*. Feb 11;88(2):173–82.
64. Purcell S, Neale B, Todd-Brown K, Thomas L, Ferreira MA, et al. (2007) PLINK: a tool set for whole-genome association and population-based linkage analyses. *Am J Hum Genet*. Sep;81(3):559–75.